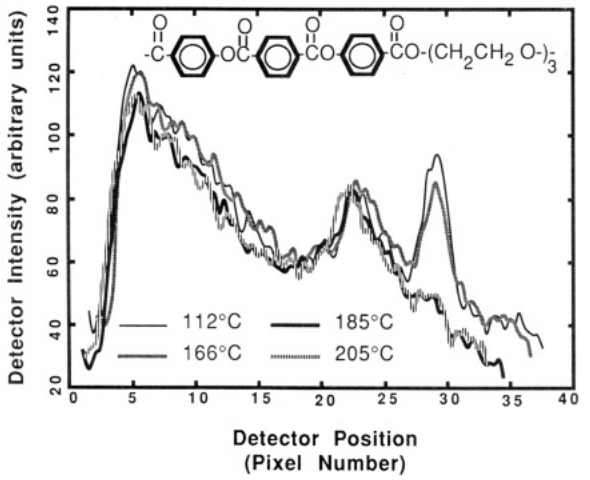

Figure 5. Recorded WAXD spectra of HTH-3 at (a) 112, (b) 166, (c) 185, and (d) 205 °C.

the extended monomeric repeat distance and may be indicative of a smectic C mesophase.

In contrast to the behavior of BP6, polymer HTH-3 is a semicrystalline polymer that exhibits both a very sharp melting transition and a pronounced clearing transition by DSC.[3] Also previously noted is an intermediate transition associated with a smectic–nematic phase transition. All transitions have been readily observed by optical microscopy. Describing the results of the dynamic X-ray studies of HTH-3 powder, Figure 5 shows the recorded intensity versus pixel position taken at four temperatures. The temperature range of observation was from the crystalline solid and the lower temperature smectic mesophase. As shown in the figure, the peak at pixel number 30 (0.45 nm) disappeared between 166 and 185 °C. Over this temperature range the melting transition took place and with this polymer we can therefore correlate DSC and dynamic X-ray behavior. Note that the peak at pixel number 7 (2.5 nm) did not change nor did the peak at pixel number 23. The latter peak is associated with the Mylar sample holder. The inner ring is associated with the smectic mesophase of HTH-3 and is qualitatively different than the inner ring of BP6. HTH-3 has previously been assigned a higher order smectic phase whereas we believe that BP6 has a smectic C mesophase.

The use of synchrotron radiation to study LCPs enables several types of experiments not previously possible. Not only may the phase transitions and biphasic behavior be observed in real time as the temperature is changes as discussed in the present paper, but the diffractograms can be recorded on a time scale which makes determination of the transition rates possible. We are presently studying the phase transitions in these and other LCPs and will report the results of such investigations in due course.

Acknowledgment. We thank the Cornell Materials Science Center (MSC) funded through NSF for financial support, use of the MSC facilities, and a fellowship for A.D. Financial assistance from the AT&T Foundation is greatly appreciated. We also thank the Cornell High Energy Synchrotron Source (CHESS) funded through NSF DMR 84-12465 for use of the facility. Finally, we thank Scott McNamee, Don Buckley, and Professors Ed Kramer and David Grubb for help with the CHESS run.

Registry No. BP6, 117939-37-4; HTH-3, 84329-77-1.

References and Notes

(1) Delvin, A.; Ober, C. K. *Polym. Bull.* **1988**, *20*, 245.
(2) Delvin, A.; Ober, C. K.; Bluhm, T. L. *Polym. Mater. Sci. Eng.* **1988**, *58*, 1029.
(3) Galli, G.; Chiellini, E.; Ober, C. K.; Lenz, R. W. *Makromol. Chem.* **1982**, *183*, 2693.

A. Delvin and C. K. Ober*
Materials Science & Engineering
Cornell University, Ithaca, New York 14853

T. L. Bluhm
Xerox Research Centre of Canada, 2660 Speakman Dr.
Mississauga, ON L5K 2L1 Canada

Received August 23, 1988

Fourier Transform Raman Studies of Secondary Structure in Synthetic Polypeptides

The importance of α-helical and the β-sheet structures on the function of both fibrous and globular proteins is well established. What is less well-known is the interrelated role of primary and secondary structures and how that influences the tertiary structure responsible for protein function. Energy calculations do not yet have the sophistication to resolve this puzzle, but some progress is being made at the experimental forefront particularly with the advent of a new technique known as Fourier transform Raman spectroscopy (FT Raman) which is described herein.

In the structural characterization of biomolecules, Raman spectroscopy has always been the technique of choice due to the problems associated with obtaining an infrared (IR) spectrum in native (usually aqueous) environments.[1] In addition, Raman spectroscopy is a noninvasive technique since usually no change in the sample or its environment occurs during structural characterization. Thus, molecules in solution pose no more of a problem than an opaque solid, and in both cases after a Raman investigation, neither the initial molecular structure nor the morphology has been altered.

On the less positive side, a Raman spectrum of a biopolymer or a protein is often unobtainable using visible excitation due to the presence of a fluorescent impurity.[2] Absorption by this impurity leads to electronic transitions followed by emission which is not spontaneous but occurs over a time interval through a manifold of intermediate states. This fluorescent emission is so efficient (high quantum yield) that its intensity will completely or, at best, partially obscure the Raman spectrum of the biomolecule of interest. In cases where the impurity chromophore does not fluoresce, it may cause local heating due to photon absorption which could subsequently lead to degradation or denaturation if the biomolecule is a protein.

Recently Raman spectroscopy has entered the Fourier domain using cw Nd:YAG excitation in the near IR at 1.064 μm.[3,4] Although photons with such a low energy cannot excite fluorescence, they still give rise to Raman scattering as indicated in Figure 1a. As shown, the frequency regime of the Stokes-shifted Raman scattering using a Nd:YAG laser is considerably lower than that using argon ion excitation. In fact, the Stokes FT Raman spectrum occurs on the lower end of the frequency region, usually referred to as the near infrared. In this region, standard Fourier transform IR (FTIR) instruments have been routinely used to make IR transmission measurements for more than 20 years. It soon became obvious that the conventional Raman dispersion spectrometer which is used for spectral analysis in the visible should be replaced by the higher throughput, multiplex FTIR instrument for analysis of Raman scattering in the near infrared. The result is schematically illustrated in Figure 1b. As

0024-9297/89/2222-0500$01.50/0

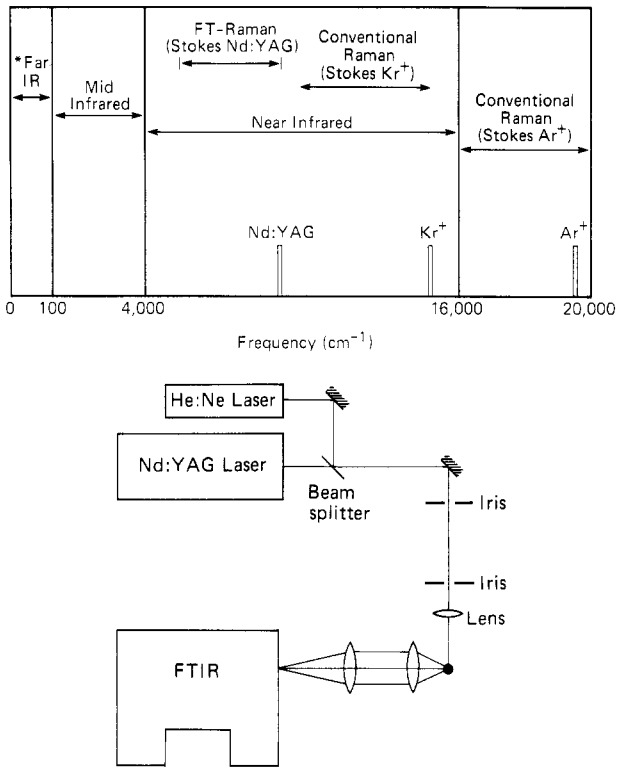

Figure 1. (a) Frequency diagram indicating location of visible and near IR laser excitation sources for Raman scattering. (b) Schematic illustration of an FT Raman instrument using transmissive collection optics.

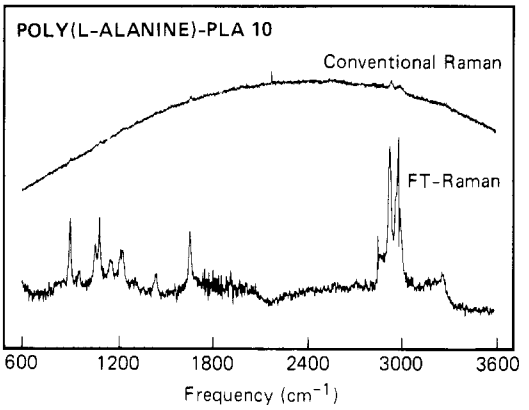

Figure 2. Comparison of conventional (upper) and FT Raman (lower) spectra of PLA-10 (powdered samples).

usual, the scattered light is collected by using standard optics, but then it is brought into the FTIR whose IR lamp has been removed. Thus, the Raman-scattered light is now the source for the FTIR, and upon Fourier transformation of the resulting interferogram, the Raman spectrum is obtained. In general, the inherent advantages of using interferometry rather than spectrometry have long been realized[5] and hence have provided an impetus for the movement of FT Raman spectroscopy in this direction.

One inherent disadvantage of this technique is the weaker scattering which occurs in the near infrared due to the inverse relationship of the Raman scattering factor on the fourth power of the wavelength. In many cases,[4] this can be compensated for by using higher incident laser powers. In our system shown in Figure 1b, a second problem has been averted by making a visible HeNe laser colinear with the Nd:YAG laser to aid sample positioning and alignment since the beam at 1.064 μm is invisible.

The implications of the FT Raman technique for the study of biomolecules is far reaching. A typical example

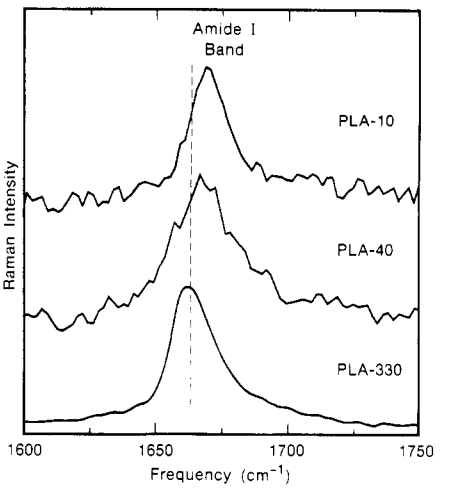

Figure 3. Amide I region of PLA-10, PLA-40, and PLA-330.

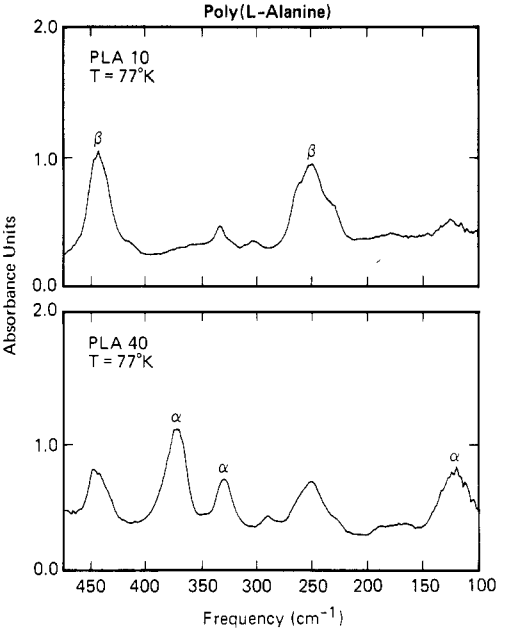

Figure 4. Far infrared transmission spectra of PLA-10 and PLA-40 at 77 K. Identical spectra were obtained at 300 K with slightly broader band shapes.

is illustrated in Figure 2 where a conventional Raman spectrum of a poly(L-alanine) oligomer containing 10 peptide units (PLA-10) is compared with the spectrum obtained by using the FT Raman technique. The fluorescent background observable in the former due to the presence of an impurity resulting from the synthetic procedure completely obscures any Raman bands. In contrast, by use of laser excitation at 1.064 μm accompanied by analysis with an FTIR, no such background is present, and a number of medium-to-strong Raman bands can be easily observed.

In an attempt to understand the role of the peptide sequence length on secondary structure, a series of different length (10, 40, and 330) poly(L-alanine) oligomers have been studied by using the FT Raman technique. Estimates of secondary structure content of proteins and polypeptides both in crystals and solutions from an analysis of the amide I (C=O stretch) band have been reliable and shown to be sensitive to small changes.[6] Typically the amide I band for β-sheet structures is found in the 1666–1669 cm^{-1} region, while that for the α helix is usually found at 1655 cm^{-1}.[7] As shown in Figure 3, the amide I band in PLA-10 is found close to 1668 cm^{-1}, in-

dicating that it exists in the β-sheet structure in the solid state. Raman studies[2] of shorter oligomers in the presence of a significant fluorescent background also found that these existed in a β-sheet structure. In contrast, the spectrum of PLA-40 reveals that amide I has shifted considerably to lower frequency, indicating that PLA-40 contains a significant amount of α-helical structure. This becomes clear in the PLA-330 spectrum where amide I is found at 1655 cm^{-1} since it is known from X-ray measurements that polypeptides which exist in the α-helical conformation have amide I bands at this position. Confirmation of these results have been obtained in the far infrared region of the spectrum where low frequency motions characteristic of α-helical and β-sheet structure are found. As shown in Figure 4, strong bands at 440 and 240 cm^{-1} characteristic of β structure are found in PLA-10, whereas the spectrum of PLA-40 is dominated by features at 375, 335, and 120 cm^{-1} attributable to the α-helical conformation.[8]

Hence, it becomes clear that the secondary structure of oligopolypeptides depends on the sequence length. In relatively short lengths (5–10 units), a β-sheet structure is preferred. However, as the sequence length increases, there is a definite preference energetically for the conformation to adopt that of an α-helix. Certainly by the time the chain length has increased to 40 units, a significant amount of α-helical content is present.

Thus, it is apparent that the FT Raman technique can provide important structural information on biomolecules whose spectra were previously unattainable due to the presence of fluorescence. However, it also continues to show considerable promise for investigating biologically relevant materials which contain chromophores as an intrinsic part of their structure and hence degrade when exposed to visible light.

Registry No. Poly(L-alanine), 25191-17-7; poly(L-alanine), SRU, 25213-34-7.

References and Notes

(1) Koenig, J. L.; Sutton, P. L. *Biopolymers* **1969**, *8*, 167.
(2) Sutton, P.; Koenig, J. L. *Biopolymers* **1970**, *9*, 615.
(3) Hirschfeld, T.; Chase, D. B. *Appl. Spectrosc.* **1986**, *40*, 1079.
(4) Zimba, C. G.; Hallmark, V. M.; Swalen, J. D.; Rabolt, J. F. *Appl. Spectrosc.* **1987**, *41*, 721.
(5) Moller, K. D.; Rothschild, W. G. *Far Infrared Spectroscopy*; Wiley: New York, 1971.
(6) Williams, R. W.; McIntyre, J. O.; Gaber, B. P.; Fleischer, S. *J. Biol. Chem.* **1986**, *261*, 14520.
(7) Fanconi, B. *Biopolymers* **1971**, *12*, 2759.
(8) Shotts, J.; Sievers, A. J. *Biopolymers* **1974**, *13*, 2593.

V. Hallmark and J. F. Rabolt*

IBM Research Division, Almaden Research Center
650 Harry Road, San Jose, California 95120

Received August 29, 1988;
Revised Manuscript Received November 3, 1988

CORRECTION

Yoshiyuki Nishio and R. St. John Manley*: Cellulose/Poly(vinyl alcohol) Blends Prepared from Solutions in *N,N*-Dimethylacetamide–Lithium Chloride. Volume 21, Number 5, May 1988, p 1270.

The caption of Figure 1c should read: 70/30 cellulose/PVA.

Table I, as printed in the May, 1988, issue, contained errors in the heading of the columns. The correct version of the table is as follows:

Table I
Melting Temperature T_m, Crystallization Temperature T_c, Glass Transition Temperature T_g, Heat of Fusion ΔH_f, and Heat of Crystallization ΔH_c of Cellulose/PVA Blends, Measured by DSC

cellulose/PVA, w/w	1st heating		2nd heating			cooling	
	T_m, °C	ΔH_f, cal/g	T_g, °C	T_m, °C	ΔH_f, cal/g	T_c, °C	$-\Delta H_c$, cal/g
0/100	229.8	24.2	80	230.1	18.7	195.9	17.5
10/90	227.2	19.2 (21.3)[d]	82	226.8	14.7 (16.3)[d]	191.5	12.7 (14.1)[d]
20/80	226.6	16.1 (20.1)	83	224.5	12.4 (15.5)	182.8	10.9 (13.6)
30/70	223.5	11.4 (16.2)	85	220.3	9.4 (13.4)	174.1	7.7 (11.0)
40/60	222.5	7.6 (12.6)	87	212.9	6.2 (10.3)	164.3	4.6 (7.7)
50/50	217.7	4.8 (9.6)	90	205.6	4.0 (8.0)	158.4	2.6 (5.2)
60/40	211.5	3.0 (7.5)	~90[e]	197.0	2.0 (5.0)	143.7	NE
70/30	NE[b]	NE	ND	~189[e]	NE	NE	~0
80/20	NE	~0	ND	NE	~0	ND	
90/10	ND[c]		ND	ND		ND	
100/0	ND		ND	ND		ND	
70/30[a]	229.3	6.9 (23.0)	83	226.5	5.3 (17.7)	not tested	
80/20[a]	229.5	3.8 (19.0)	80	228.0	3.1 (15.5)	not tested	

[a] Mechanical mixture of both polymers as a fine powder. [b] NE = could not be estimated. [c] ND = not detected. [d] Based on weight of PVA. [e] Estimated with great uncertainty.